Angiogenesis (2019) 22:251–262
https://doi.org/10.1007/s10456-018-9654-1

ORIGINAL PAPER

# The regulatory network of miR-141 in the inhibition of angiogenesis

**Haojie Dong[1,4] · Chunhua Weng[5] · Rongpan Bai[1] · Jinghao Sheng[1,2,3] · Xiangwei Gao[1] · Ling Li[4] · Zhengping Xu[1,2,3]**

Received: 8 May 2018 / Accepted: 12 November 2018 / Published online: 21 November 2018


## Abstract

The miR-200 family, consisting of miR-200a/b/c, miR-141, and miR-429, is well known to inhibit epithelial-to-mesenchymal transition (EMT) in cancer invasion and metastasis. Among the miR-200 family members, miR-200a/b/c and miR-429 have been reported to inhibit angiogenesis. However, the role of miR-141 in angiogenesis remains elusive, as contradicting results have been found in different cancer types and tumor models. Particularly, the effect of miR-141 in vascular endothelial cells has not been defined. In this study, we used several in vitro and in vivo models to demonstrate that miR-141 in endothelial cells inhibits angiogenesis. Additional mechanistic studies showed that miR-141 suppresses angiogenesis through multiple targets, including *NRP1, GAB1, CXCL12β, TGFβ2*, and *GATA6*, and bioinformatics analysis indicated that miR-141 and its targets comprise a powerful and precise regulatory network to modulate angiogenesis. Taken together, these data not only demonstrate an anti-angiogenic effect of miR-141, further strengthening the critical role of miR-200 family in the process of angiogenesis, but also provides a valuable cancer therapeutic target to control both angiogenesis and EMT, two essential steps in tumor growth and metastasis.

**Keywords** miR-141 · miR-200 family · Angiogenesis · Regulatory network

## Introduction

Angiogenesis, the growth of new capillary vessels from existing vasculature, plays an essential role in a number of physiological and pathological processes, including embryonic development, wound healing, inflammation, and tumor growth and metastasis [1–3]. MicroRNAs (miRNAs) are a class of highly conserved non-coding small RNA molecules that post-transcriptionally down-regulate target gene expression through translational repression or mRNA degradation [4]. Accumulating evidence suggests that miRNAs play a critical role in various bioprocesses, including angiogenesis and tumor progression [5–7].

The miR-200 family of miRNAs contains five members, and organized into two clusters: miR-200b/a/429 and miR-200c/141. This family has been well documented to play an essential role in tumor maintenance and malignant metastasis by targeting several central inducers of the epithelial-to-mesenchymal transition (EMT) process, such as *ZEB1, ZEB2*, and *SLUG* [8–10]. Additional studies have shown that some miR-200 family members also regulate the process of angiogenesis [11–13]. The role of miR-141 in angiogenesis, however, remains unclear as contradicting lines of evidence

**Electronic supplementary material** The online version of this article (https://doi.org/10.1007/s10456-018-9654-1) contains supplementary material, which is available to authorized users.

✉ Zhengping Xu
zpxu@zju.edu.cn

1 Institute of Environmental Medicine, and Cancer Center of the First Affiliated Hospital, Zhejiang University School of Medicine, 866 Yuhangtang Road, Hangzhou 310058, China

2 Collaborative Innovation Center for Diagnosis and Treatment of Infectious Diseases, Zhejiang University, Hangzhou 310003, China

3 Program in Molecular and Cellular Biology, Zhejiang University School of Medicine, Hangzhou 310058, China

4 Department of Hematological Malignancies Translational Science, Beckman Research Institute, City of Hope Medical Center, Duarte, CA 91010, USA

5 Kidney Disease Center of the First Affiliated Hospital, Zhejiang University School of Medicine, Hangzhou 310003, China

suggest that miR-141 could promote [14, 15] or inhibit [16] angiogenesis. For example, xenografts from Kras-transformed mouse fibroblasts that overexpressed miR-141 developed more large blood vessels than those that did not [14]. In line with this, non-small cell lung cancer (NSCLC) patient samples with high levels of miR-141 expression had greater microvessel density than those with less miR-141 expression [15]. In contrast, miR-141 has been shown to reduce microvessel density and primary tumor growth in a basal-like breast cancer model [16]. These studies, however, were conducted in tumor-based models or patient samples with complicated microenvironments and various cell–cell interactions that prevent the evaluation of the direct role of miR-141 in vascular endothelial cells.

In this study, we explored the role of miR-141 in angiogenesis using several endothelial angiogenesis models both in vitro and in vivo. We demonstrated that miR-141 inhibits endothelial cell proliferation, migration, and tube formation in vitro, as well as angiogenesis in vivo. In silico analysis and functional studies revealed that miR-141 represses angiogenesis through multiple targets, including *NRP1, GAB1, CXCL12β, TGFβ2*, and *GATA6*. Literature reviewing and bioinformatics analysis indicated that these targets are located in different cell components and may constitute a "3D" regulatory network through which miR-141 modulates different steps of angiogenesis. Taken together with previous findings regarding the involvement of miR-141 in EMT regulation, our results shed light on the critical role of miR-141 in the processes of EMT and angiogenesis, two essential steps in tumor growth and metastasis. Thus, our findings may support the development of miR-141-based tumor therapy.

## Materials and methods

### Cell culture

Human primary umbilical vein endothelial cells (HUVECs) were isolated from the human umbilical cords of healthy newborns, as described previously [17]. The use of human umbilical cords was approved by the Ethics Committee of Zhejiang University School of Medicine (Approval ID 2010-121). HUVECs were cultured in modified endothelial cell growth medium containing 52% M199 medium (Life Technologies, Carlsbad, CA, USA), 36% Human Endothelial-SFM (Life Technologies), 10% fetal bovine serum (FBS, Life Technologies), and 15 μg/ml endothelial cell growth supplement (ECGS, Millipore, Billerica, MA, USA). HUVECs were used in the experiments between passages 3 and 8. HEK293T and HEK293T/17 cells were maintained in Dulbecco's Modified Eagle's Medium (Life Technologies) supplemented with 10% FBS (Hyclone, Logan, UT, USA). All cells were incubated at 37 °C in an incubator with a humidified atmosphere of 5% $CO_2$.

### Plasmid construction

For dual-luciferase reporter assays, the regions of the 3′UTR sequences containing the predicted miR-141 binding sites of *CXCL12β, GAB1, GATA6, NRP1, RUNX1*, or *TGFβ2* were cloned into the *Xho*I and *Not*I sites of psiCHECK-2 dual-luciferase reporter vectors (Promega, Madison, WI, USA). The cloned regions are listed in Supplementary Table S1. Site-direct mutagenesis of miR-141 binding site was performed using the *FAST* Mutagenesis System (TransGen Biotech, Beijing, China) as described in Supplementary Table S2. The tested 3′UTR regions of *CXCL12β, GATA6*, and *RUNX1* were synthesized by FulenGen Co. (Guangzhou, China). To construct the miR-141 lentivirus expression plasmid, the pri-miR-141 sequence was PCR amplified from HUVEC genomic DNA and cloned into the *Xba*I and *Eco*RI sites of a pMIRNA1 vector (System Biosciences, Palo Alto, CA, USA). All primers used are listed in Supplementary Table S3. All constructs were verified using DNA sequencing.

### Lentivirus packaging and transduction

The miR-141 lentivirus was produced by co-transfecting HEK 293T/17 cells with pMIRNA1-miR-141, psPAX2, and pMD2.G. Transfection was carried out using Lipofectamine 2000 (Life Technologies) according to the manufacturer's protocol. Forty-eight hours after transfection, supernatant containing the lentivirus was harvested, centrifuged at 600×*g* for 5 min, filtered through a 0.45-μm PES filter, aliquoted, and stored at − 80 °C. Viral titer was determined using serial dilution and fluorescence detection. Transduction was carried out in the presence of 10 μg/ml polybrene (Millipore). The supernatant was removed 24 h after transduction, and GFP-positive cells were examined under a fluorescence microscope. The GAB1 lentivirus was produced using the same procedure described above.

### RNA oligoribonucleotides and transfection

HUVECs were grown to 60–70% confluence before transfection with siRNAs, miRNA mimics (miR-141 mimic or agomir-141) or miRNA inhibitor (miR-141 inhibitor) at 40 nM. Transfections were performed with Lipofectamine RNAiMAX Transfection Reagent (Life Technologies) according to the manufacturer's protocol. The negative control RNAs for siRNAs (NC), miRNA mimics (NC or agomir-NC), and miRNA inhibitor (NC inhibitor) have no genetic homology with human or mouse genomic sequences. The siRNAs used are listed in Supplementary Table S4. All

siRNAs, miRNA mimics, and miRNA inhibitor were purchased from GenePharma Co. (Shanghai, China).

### RNA extraction, reverse transcription PCR, and real-time PCR

Total RNA was extracted from cultured cells using Trizol reagent (Life Technologies) and a Direct-zol-RNA-Mini-Prep kit (ZYMO Research, Irvine, CA, USA). RT-PCR was performed using TaqMan primers (Life Technologies). U6 small nuclear RNA was used as an internal control. To quantify mRNA levels of candidate target genes, reverse transcriptase reactions were carried out with 500 ng total RNA and M-MLV Reverse Transcriptase (Life Technologies). The real-time PCR analyses of *CXCL12β, GAB1, GATA6, NRP1, RUNX1, TGF*β2, and *GAPDH* genes were performed using a SYBR *Premix Ex Taq* kit (TAKARA Bio, Shiga, Japan). The real-time PCR primers used are listed in Supplementary Table S5. All primers were synthesized by Sangon Co. (Shanghai, China). All mRNA levels were normalized to the *GAPDH* mRNA level. Data were analyzed using the $^{\Delta\Delta}C_t$ method.

### Western blot analysis

Transfected HUVECs were harvested and lysed in RIPA buffer [50 mM Tris, pH 7.4, 150 mM NaCl, 1% Triton X-100, 1% sodium deoxycholate, 0.1% SDS, and protease inhibitor cocktail (Roche Diagnostics, Indianapolis, IN, USA)] for 30 min on ice. Cell lysates were separated by electrophoresis in 10–15% SDS-polyacrylamide gels and blotted onto nitrocellulose membranes. Western blots were performed using the antibodies listed in Supplementary Table S6. The IRDye 800CW-labeled goat anti-rabbit or anti-mouse secondary antibody (Li-COR Biosciences, Lincoln, NE, USA) was visualized and quantified using an Odyssey Infrared Imaging System (LI-COR Biosciences).

### Dual-luciferase reporter assay

Luciferase reporter assays were performed in HEK293T cells. Twenty-five thousand cells per well were seeded in a 96-well plate. After 24 h, the cells were co-transfected with 5 pmol miR-141 mimic and 25 ng psiCHECK2-X plasmids, where X stands for the predicted target genes using Lipofectamine 2000 (Life Technologies), according to the manufacturer's protocol. Cell extracts were prepared using 1 × Passive Lysis Buffer (Promega) 48 h after transfection, and luciferase activity was measured using the Dual-Luciferase Reporter Assay System kit (Promega). *Renilla* luciferase activity was normalized to *Firefly* luciferase activity (RL/FL) for each group before comparison with the corresponding control group.

### Cell proliferation assay

A Cell Counting Kit-8 (CCK-8, Dojindo, Kumamoto, Japan) was used to measure proliferation of transfected HUVECs, according to the manufacturer's protocol. Twenty-four hours after transfection, HUVECs were harvested and seeded in 96-well plates at a density of 2000 cells per well. The baseline was determined when the cells adhered to the plate. Cell numbers were detected by measuring OD450 in a microplate reader at days 1, 2, 3, and 4 after seeding.

### Real-time cell migration assay using the xCELLigence system

The xCELLigence system is a versatile device that quantitatively measures the migratory ability of cells in real time without exogenous labels [18]. HUVECs were harvested and seeded 10,000 cells/well in a cell invasion and migration plate (CIM-plate 16), and the real-time cell migration assay was performed in the xCELLigence RTCA DP Analyzer (Roche).

### Wound healing assay

HUVECs were seeded in six-well plates and cultured to a confluent monolayer. Three separate wounds were scratched using a pipet tip and cells were rinsed with culture medium. Pictures of the wound were taken at the same position under a microscope (Nikon *Ts-i*, Nikon, Shinagawa, Japan) at 0 h and 12 h. Migration ability was analyzed by quantifying the wound area using Image Pro Plus software (IPP, Media Cybernetics, Rockville, MD, USA).

### Tube formation assay

A tube formation assay on Growth Factor Reduced (GFR) Matrigel (BD Biosciences, Franklin Lakes, NJ, USA) was employed to evaluate capillary-like structure formation by HUVECs. At 24-h post-transfection, HUVECs were washed twice with serum-free medium, then 3500 cells were suspended in 50 µl serum-free medium and plated on µ-slide angiogenesis plates (ibidi GmbH, Martinsried, Germany) coated with 10 µl GFR Matrigel. The extent of tube formation was assessed 6–8 h after seeding. IPP software was used to quantify tube length and branch points.

### In vivo matrigel plug assay

The in vivo matrigel plug assay was performed as described previously [19] with some modifications. Briefly, 100 µM agomir-141 or agomir-NC (GenePharma Co.) was resuspended in 30 µl PBS and mixed with 500 µl Matrigel Basement Membrane Matrix (BD Biosciences) containing 15

units of heparin (Sigma-Aldrich). The matrigel mixture was injected subcutaneously into 5–7-week-old C57 BL/6 mice along the abdominal midline. After 6–8 days, the animals were sacrificed and plugs removed. Angiogenesis ability was quantified by immunohistochemical staining of blood vessels, as described below. Mice were treated and cared for according to guidelines and protocols approved by the Medical Experimental Animal Care Commission of Zhejiang University (Approval ID ZJU201402-1-01-033).

### Immunohistochemistry

Dissected matrigel plugs were fixed in 10% formalin and embedded in paraffin. 4-μm-thick sections were cut and subjected to immunohistochemical staining. Neovessels were stained with a rabbit anti-CD31 antibody (ab28364; Abcam, Cambridge, UK). Sections were deparaffinized with xylene, rehydrated in ethanol, and boiled in 10 mM citrate buffer (pH 6.0) for 30 min for antigen retrieval. Endogenous peroxidase was blocked by treatment with 3% $H_2O_2$ in methanol for 10 min. Slides were then blocked in goat serum for 30 min at room temperature, incubated with the anti-CD31 primary antibody at a dilution of 1:100 at 4 °C overnight, incubated with anti-rabbit secondary antibodies for 1 h, and visualized using the EnVision System (DAKO Corporation, Carpinteria, CA, USA) and diaminobenzidine (DAB) substrate kit (Life Technologies). Slides were counterstained with hematoxylin. Negative controls were obtained through the same process but omitting primary antibodies. CD31-positive vessels were counted in the five most highly vascularized areas of each section at ×200 magnification.

### Statistical analysis

The data are presented as the mean ± SD or percentages of the control ± SD from at least three independent experiments. The cell migration curve was analyzed using a two-way ANOVA analysis. miRNA or mRNA expression in more than two groups and cell proliferation at different time points were compared using one-way ANOVAs. Comparisons of two groups were conducted using two-tailed unpaired Student's *t* tests. *N* denotes the number of mice used for in vivo experiments. All analyses were performed using GraphPad Prism 5 (Graph Software, Inc., San Diego, CA, USA). $P < 0.05$ was considered statistically significant.

## Results

### All the members of miR-200 family inhibit HUVEC tube formation in vitro

The tube formation assay, one of the most widely used assays to model the process of angiogenesis in vitro, was employed to evaluate the activity of the five members of the miR-200 family in angiogenesis. Interestingly, in addition to verifying the previously reported inhibition of angiogenesis by miR-200a, miR-200b, miR-200c, and miR-429, our study showed that miR-141 also inhibited HUVEC tube formation in vitro (Fig. 1). This result indicates that all the five members of miR-200 family have the potential to suppress angiogenesis.

### miR-141 inhibits angiogenesis in vitro

We next performed a series of in vitro analyses to clarify the role of miR-141 in the process of angiogenesis. First, we transiently transfected HUVECs with a synthetic miR-141 mimic to overexpress miR-141 or a miR-141 inhibitor to block endogenous miR-141 function. HUVEC proliferation assay showed that overexpression of miR-141 repressed the proliferation of HUVECs (Fig. 2a), whereas suppression of endogenous miR-141 promoted proliferation (Fig. 2b). To confirm the suppressive effect of miR-141 in HUVEC proliferation, we transduced HUVECs with a lentivirus expressing pri-miR-141 to generate mature miR-141 using the intracellular miRNA biogenesis system (Fig. S1a, b). Unexpectedly, lentiviral-induced overexpression of miR-141 was more than 300-fold that of baseline expression. This level of overexpression is not normally expected in the cells; therefore, it may have had some unintended consequences on cell function. However, control and miR-141 lentiviruses infected similar numbers of cells and resulted in similar levels of GFP fluorescence (Fig. S1a). Overall, this experiment confirmed that overexpression of miR-141 prominently inhibits HUVEC proliferation (Fig. S1c).

To detect the effects of miR-141 in HUVEC migration, we analyzed cell migration using an xCELLigence real-time migration assay, as well as a wound healing assay, after transfection with the miR-141 mimic and inhibitor described above. Both assays revealed that overexpression of miR-141 repressed migration, whereas suppression of endogenous miR-141 enhanced migration (Figs. 2c–f, S1d–f). Notably, the formation of capillary-like structures by HUVECs was reduced dramatically when miR-141 was overexpressed (Figs. 2g–i, S1g–i). In contrast, blocking the activity of miR-141 with the miR-141 inhibitor resulted

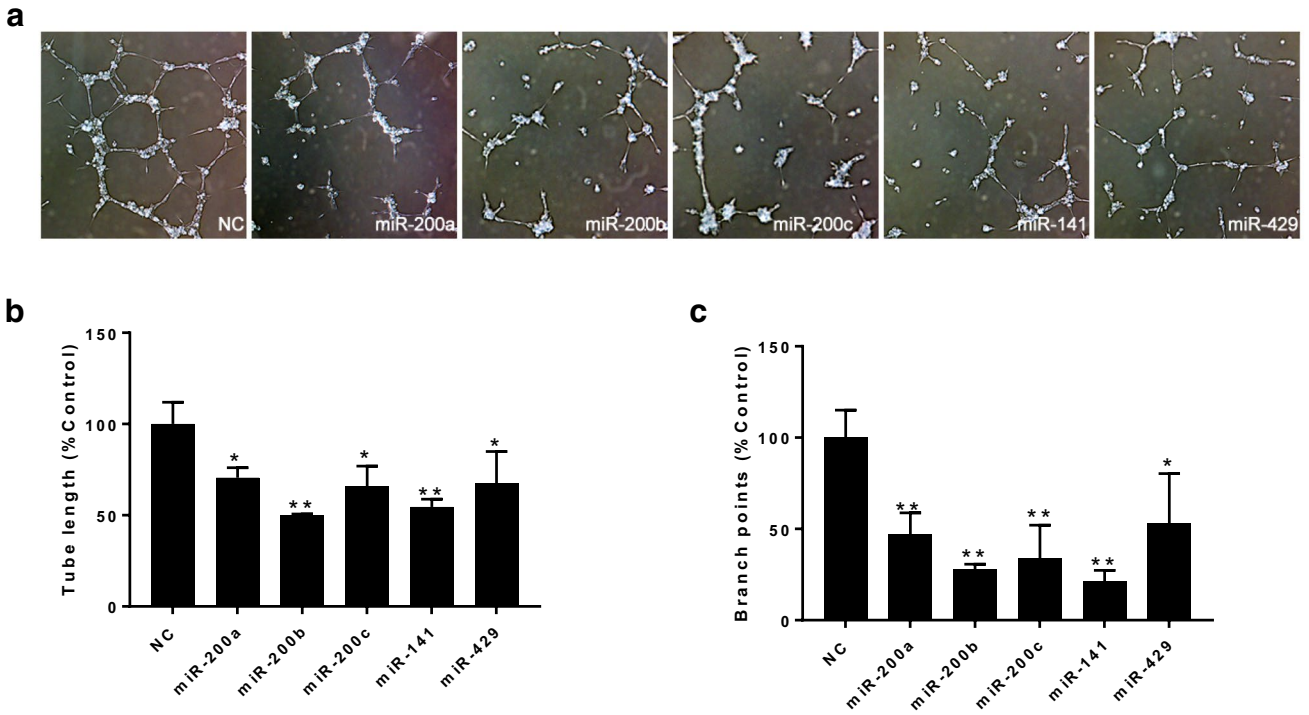


**Fig. 1** The entire miR-200 family inhibits HUVEC tube formation. HUVECs transfected with individual miR-200 family member mimics were harvested and reseeded into matrigel-coated μ-slide angiogenesis plates for tube formation assays. **a** Representative pictures of HUVEC tube formation in the presence of miR-200 family mimics or a negative control (NC). Tube length (**b**) and branch points (**c**) were analyzed to evaluate angiogenic activity of each member. $^{*}P<0.05$, $^{**}P<0.01$

in enhanced tubular structure formation by HUVECs (Fig. 2g–i). Together, these in vitro results suggest that miR-141 negatively regulates angiogenesis through the inhibition of multiple bio-events.

## miR-141 inhibits angiogenesis in vivo

We used a matrigel plug assay to further validate the role of miR-141 in angiogenesis in vivo. In accordance with our in vitro results, after 6–8 days implanted in C57 BL/6 mice, control group that treated with agomir-NC had more blood vessels than agomir-141 treated group (Fig. 3a). CD31 staining of the matrigel slices showed that there were fewer microvessels in miR-141 group than in control group (Fig. 3b, c). Collectively, our data suggest that miR-141 inhibits angiogenesis both in vitro and in vivo.

## Prediction and identification of miR-141 targets involved in angiogenesis

To elucidate how miR-141 exerts its anti-angiogenic function, putative miR-141 target genes involved in controlling angiogenesis were predicted in silico using three algorithms: TargetScan [20], PicTar [21], and DIANA microT [22] (Fig. 4a). Among the 76 commonly predicted miR-141 targets, six were chosen for further validation due to their importance in angiogenesis: *CXCL12β* [23, 24], *GAB1* [25, 26], *GATA6* [27], *NRP1* [28, 29], *RUNX1* [30, 31], and *TGFβ2* [32, 33] (Fig. 4b). A dual-luciferase reporter assay revealed that co-transfection of HEK293T cells with miR-141 significantly inhibited the luciferase activity of constructs expressing the wild-type 3′UTRs of *CXCL12β, GAB1, GATA6, NRP1*, or *TGFβ2*. This inhibitory effect was abrogated when the predicted binding site in the 3′UTR was mutated (Fig. 4c). However, co-transfection with miR-141 did not influence the activity of the luciferase reporter carrying the wild-type 3′UTR of *RUNX1* (Fig. 4c). These results demonstrate that miR-141 may negatively regulate *CXCL12β, GAB1, GATA6, NRP1*, and *TGFβ2*, but not *RUNX1*, by binding to their mRNA 3′UTRs.

To confirm that miR-141 affects the expression of these targets in HUVECs, their mRNA and protein levels were analyzed by real-time PCR and western blot analysis after transfection with a miR-141 mimic. The mRNA levels of *CXCL12β, GAB1, GATA6*, and *NRP1* did not change significantly but *TGFβ2* expression was significantly reduced (Fig. 4d). Meanwhile, the protein levels of GAB1, NRP1, TGFβ2 (preproprotein of TGFβ2) and GATA6, but not RUNX1, were down-regulated after miR-141 overexpression (Fig. 4e). Because CXCL12β is a small secreted chemokine

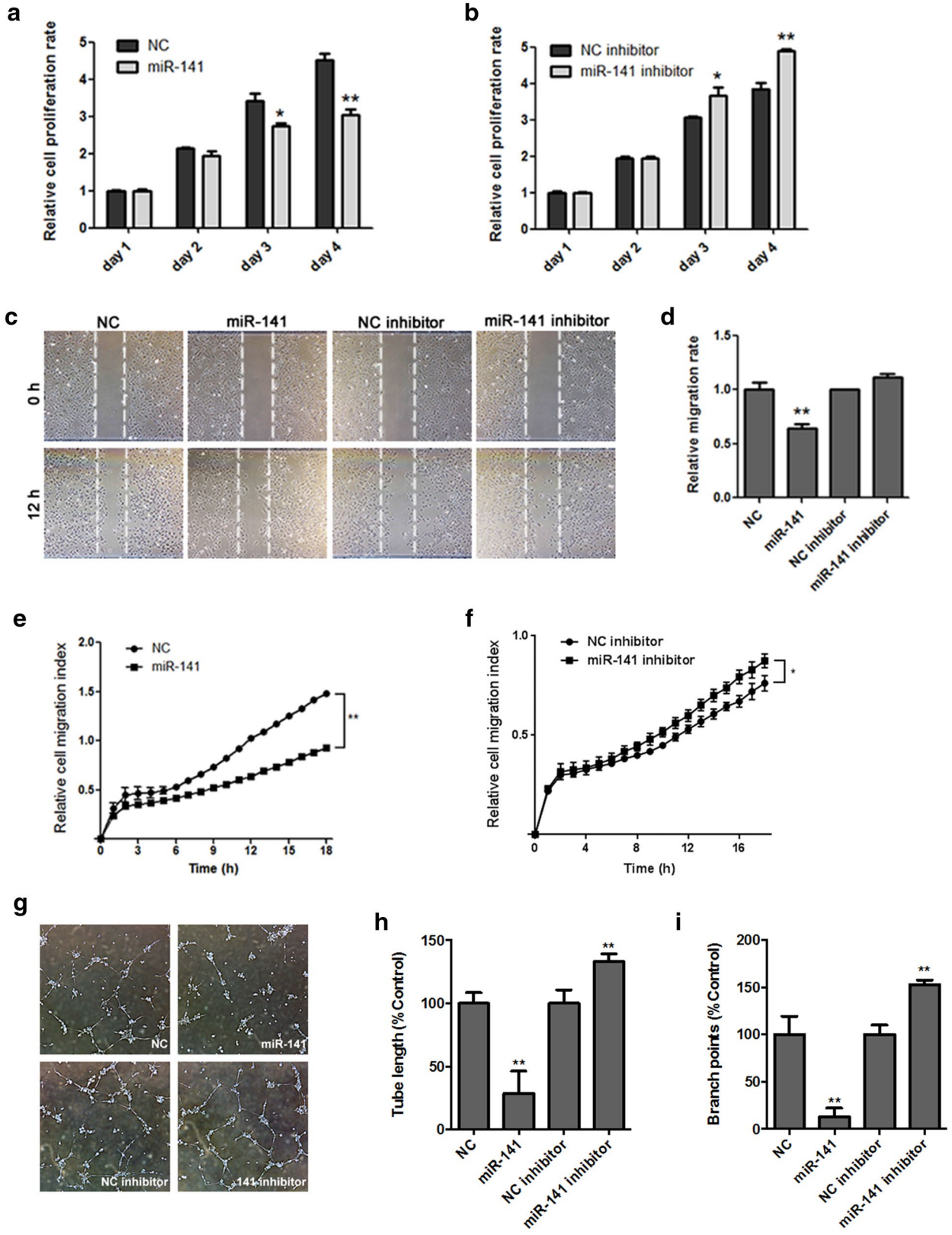
a
Relative cell proliferation rate
NC
miR-141
day 1
day 2
day 3
day 4
b
Relative cell proliferation rate
NC inhibitor
miR-141 inhibitor
c
NC
miR-141
NC inhibitor
miR-141 inhibitor
0 h
12 h
d
Relative migration rate
e
Relative cell migration index
Time (h)
f
Relative cell migration index
Time (h)
g
NC
miR-141
NC inhibitor
141-inhibitor
h
Tube length (% Control)
i
Branch points (% Control)

◂**Fig. 2** miR-141 inhibits HUVEC proliferation, migration, and tube formation in vitro. **a, b** HUVECs transfected with a miR-141 mimic (**a**) or miR-141 inhibitor (**b**) were harvested and reseeded into 96-well plates. Cell proliferation was evaluated using a CCK-8 kit on days 1, 2, 3, and 4 after reseeding. **c, d** HUVECs transfected with a miR-141 mimic or inhibitor were grown to a confluent monolayer for a wound healing assay. Dashed lines delineate the scratched wound area. Migration activity into the wound area was quantified relative to NC. **e, f** HUVECs transfected with a miR-141 mimic or inhibitor were harvested and reseeded into CIM-plates 16 for a real-time cell migration assay using the Roche xCELLigence system. Cell migration was quantified and plotted over a period of 18 h. **g** HUVECs transfected with a miR-141 mimic or inhibitor were harvested and reseeded into matrigel-coated µ-slide angiogenesis plates for tube formation assays. Representative pictures of tube formation of HUVECs are shown. Tube length (**h**) and branch points (**i**) were analyzed to evaluate angiogenic activity. $*P<0.05$, $**P<0.01$

and has been reported as the target of miR-141, we did not detect it using ELISA in this study [34]. Our findings are consistent with reports of *GAB1, CXCL12β*, and *TGFβ2* as miR-141 targets in keloid fibroblasts, colorectal cancer cells, and colonic epithelia cells, respectively [34–36], and suggest that miR-141 may repress angiogenesis by modulating the expression of *CXCL12β, GAB1, GATA6, NRP1*, and *TGFβ2* at the post-transcriptional level.

## miR-141 inhibits angiogenesis through multiple targets

To test whether the anti-angiogenic effect of miR-141 is in fact due to the down-regulation of its five angiogenesis-related targets, we conducted rescue experiments using tube formation as the detected endpoint. CXCL12β and TGFβ2, two secreted cytokines, were added directly to the medium to restore their protein levels. As the result, miR-141-eliminated capillary-like structure formation was significantly increased by 26.4% (CXCL12β rescue group) and 13.6% (TGFβ2 rescue group), with the tube length increasing from 61.0% of the NC group to 87.4% and 74.6%, respectively (Fig. 5a–c). GAB1 is a cytosolic protein, so we supplemented its expression using a lentiviral approach. After successfully boosting cellular GAB1 levels (Fig. 5g), miR-141-suppressed tube length rose from 17.1% of the empty vector-treated NC control group to 58.2% (41.1% increase) (Fig. 5d–g). Unfortunately, we failed to express GATA6 and NRP1 in HUVECs, and could not complete their rescue experiments. However, previous studies have reported that silencing or neutralizing these targets inhibits angiogenesis [27, 33, 37–39]. To confirm our findings, we knocked down the five miR-141 targets using siRNAs in HUVECs transfected with the miR-141 inhibitor, and

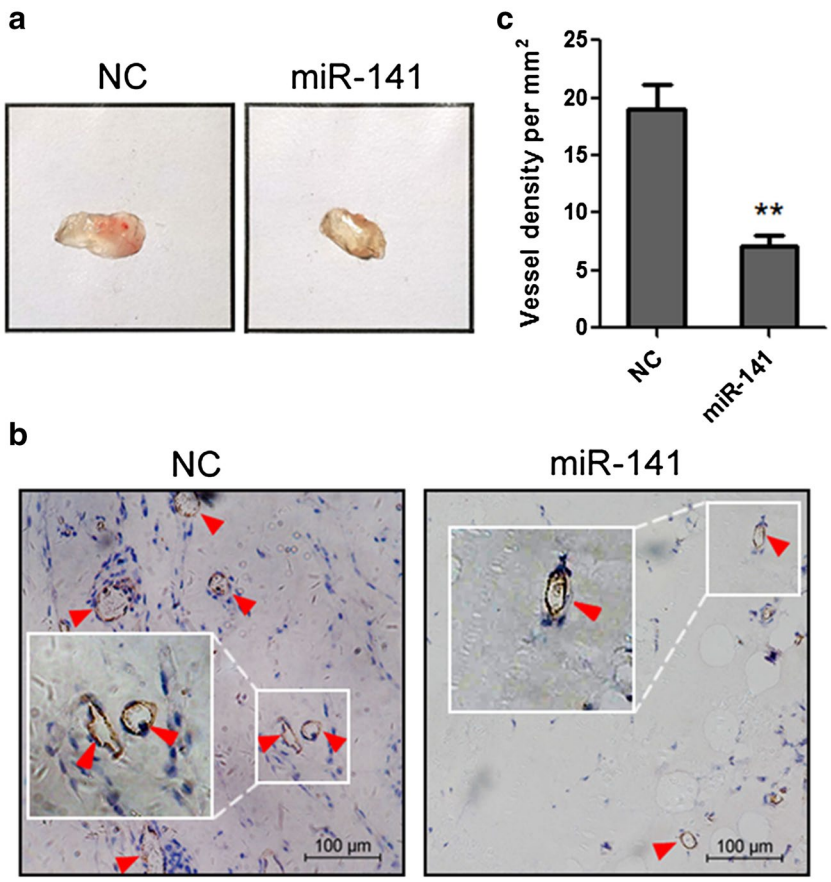


**Fig. 3** miR-141 inhibits angiogenesis in vivo. Matrigel containing agomir-141 (miR-141) or agomir-NC (NC) was injected subcutaneously along the abdominal midline of C57 BL/6 mice. Matrigel plugs were harvested 6–8 days after implantation, fixed, sliced, and immunohistochemically stained with an anti-CD31 antibody. **a** Representative pictures of the matrigel plugs harvested from mice. **b** Representative micrographs of matrigel plug slices immunohistochemically stained with an anti-CD31 antibody. Red arrows indicate the CD31 positive vessels. White boxes indicate enlarged areas of formed vessels. **c** Quantification of vessel density in matrigel plugs based on CD31 staining. $N=5$. Scale bar 100 µm. $*P<0.05$, $**P<0.01$

a

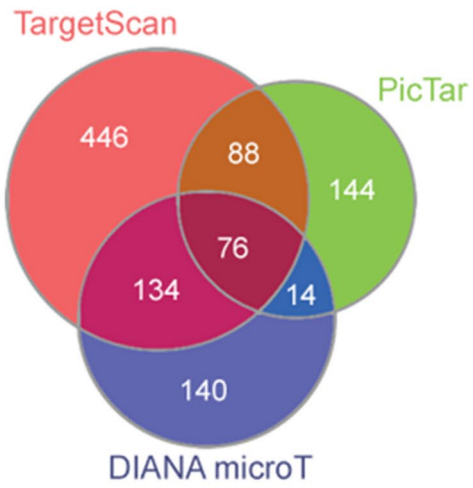


b

| Predicted target gene | Number of miR-141 binding sites | Previously reported miR-141 targets (number of sites) |
|---|---|---|
| CXCL12β | 2 | Yes(2) [34] |
| TGFβ2 | 2 | Yes(1) [35] |
| GAB1 | 2 | Yes(1) [36] |
| GATA6 | 1 | No |
| NRP1 | 1 | No |
| RUNX1 | 1 | No |

c

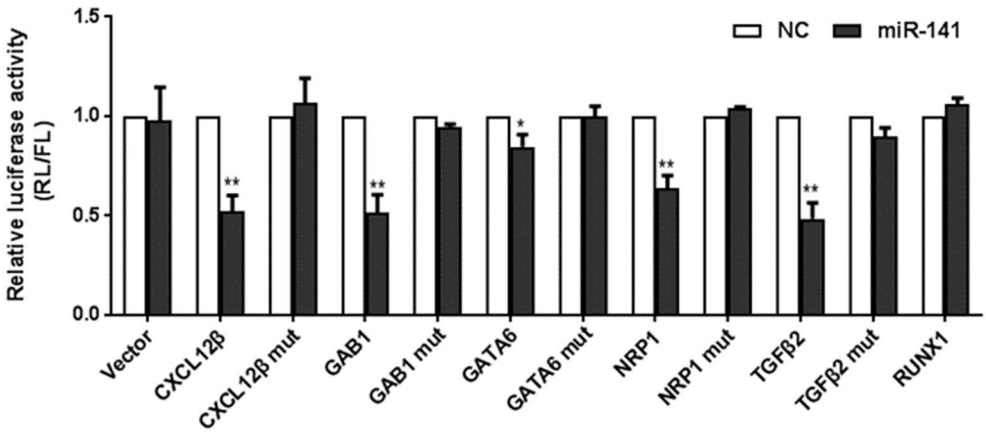


d

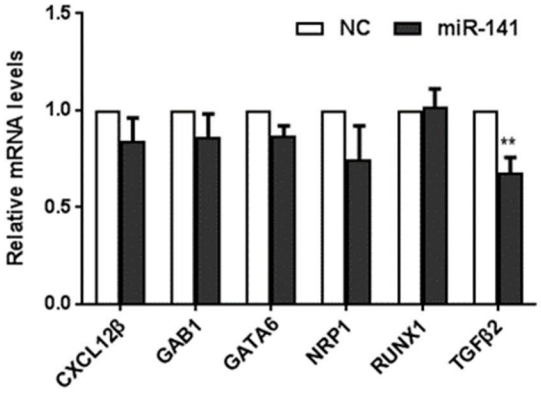


e

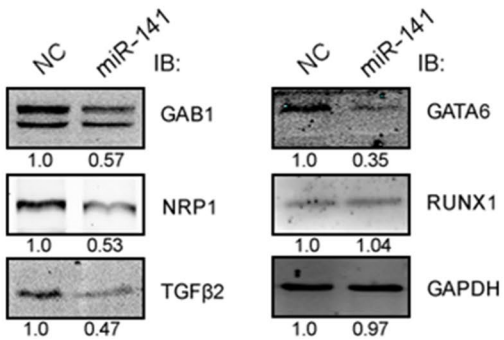


**Fig. 4** Identification of miR-141 target genes involved in angiogenesis. **a** Venn diagram of miR-141 targets predicted by three different algorithms with 76 commonly hits. **b** Gene ontology and functional analysis revealed 6 commonly predicted targets that are associated with angiogenesis. **c** HEK293T cells were co-transfected with a miR-141 mimic and psiCHECK2 plasmid containing luciferase and the normal or mutated binding site of each putative miR-141 target. Cells were lysed, and the ability of miR-141 to target the binding site was analyzed based on luciferase activity. **d** Real-time PCR analysis of the mRNA levels of each predicted miR-141 target gene after transfection with a miR-141 mimic. **e** Western blot analysis (IB) of the protein level of each predicted miR-141 target gene after transfection with a miR-141 mimic. Mean protein expression levels, relative to NC, are noted below each image. GAPDH was included as a loading control. Data shown are mean ± SD of three independent experiments. $^{*}P < 0.05$, $^{**}P < 0.01$

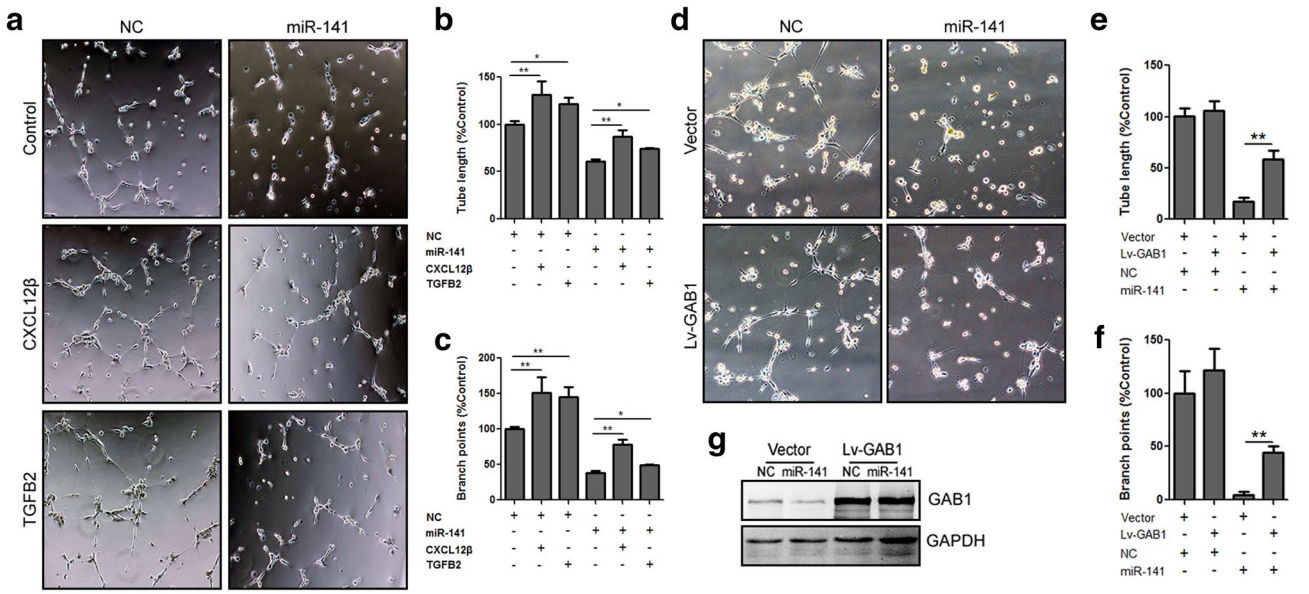


**Fig. 5** miR-141 inhibits angiogenesis through multiple targets. **a** Representative images of HUVECs after transfected with a miR-141 mimic, harvested, and reseeded into matrigel-coated μ-slide angiogenesis plates with or without 100 ng/ml CXCL12β or 0.5 ng/ml TGFβ2. Tube length (**b**) and branch points (**c**) were analyzed to evaluate angiogenic activity. **d**–**f** HUVECs transduced with lentivirus-GAB1 (Lv-GAB1) or a control vector (vector) were transfected with a miR-141 mimic, and tube formation was assessed. **g** Western blot analysis of GAB1. $^{*}P < 0.05$, $^{**}P < 0.01$

evaluated the HUVEC tube formation. Our results showed that down-regulation of these targets antagonized miR-141 inhibitor-promoted tube formation to varying degrees (Fig. S2). The inhibitory effects of siCXCL12β and siGAB1 were significantly greater than those of the other three siRNAs (Fig. S2c). Taken together with our rescue experiment results, these data suggested that CXCL12β and GAB1 might contribute more than the other targets to the miR-141 angiogenesis regulatory network. In sum, we verified that miR-141 inhibits angiogenesis through multiple targets, including *GAB1, CXCL12β, TGFβ2, GATA6*, and *NRP1* in our model.

## Discussion

miR-141 is a tumor-related miRNA, found to be not only aberrantly expressed in many malignant tumors, but an active participant in various tumorigenic processes, including EMT and tumor proliferation, migration, and invasion [40]. However, the role of miR-141 in angiogenesis has remained ambiguous. In this study, we adopted several in vitro and in vivo endothelial cell-based angiogenesis models to clearly demonstrate that miR-141 functions as an anti-angiogenic molecule. Furthermore, we identified *NRP1, GAB1, CXCL12β, TGFβ2*, and *GATA6* as the angiogenesis-related target genes of miR-141 in endothelial cells, and verified that miR-141 blocks angiogenesis by down-regulating these multiple target genes. Hence, we can now conclude that the entire miR-200 family inhibits angiogenesis.

Among the members of miR-200 family, miR-200b was the first member to be identified as an angiogenesis suppressor [11]. Later on, several reports showed that it directly targets *VEGFA, FLT/VEGFR1*, and *KDR/VEGFR2*, three key components of the VEGF signaling pathway [11, 41, 42]. miR-200c and miR-429, sharing same seed sequence with miR-200b, were also reported to inhibit angiogenesis by targeting the VEGF signaling pathway directly or indirectly [12, 43, 44]. In addition, miR-200a, which shares same seed sequence with miR-141, was found to repress angiogenesis through direct and indirect mechanisms by targeting IL-8 and CXCL1 secreted by the tumor endothelial and cancer cells [16]. Although data revealed that there was direct binding between miR-200a and the 3′ UTR of *IL-8* or *CXCL1*, lack of casual relationship among miR-200a, *IL-8* and *CXCL1*, and angiogenesis prevents to conclude that both genes are the real target genes of this miRNA. Here, after uncovering the inhibition function of miR-141 on angiogenesis, we adopted an in silico approach to predicate its putative target genes. Firstly, three mostly used bioinformatic algorithms (i.e., TargetScan, PicTar, and DIANA microT) were employed to extract possible target lists for each algorithm. After overlapping these hits, we obtained 76 genes as putative targets. Secondly, a functional annotation clustering analysis was carried out to analyze their involvement in angiogenesis using the DAVID bioinformatics database,

and only two genes, *NRP1* and *TGFB2*, were appeared in the angiogenesis cluster. Thirdly, we incorporated the latest gene function reports by searching literature, and further identified *GAB1, CXCL12β*, and *GATA6* as angiogenesis-related target genes of miR-141. Among these six genes, *CXCL12β, TGFβ2*, and *GAB1* have already been reported as miR-141 targets in colonic epithelia cells, colorectal cancer cells, and keloid fibroblasts, respectively [34–36]. Based on published data and our results, we have found that some miR-200 family members have common targets, whereas some have unique targets, indicating that the target genes are cell context-dependent.

Combinatorial regulation is a feature of miRNA action in various bioprocesses [45]. After carefully considering that the five identified miR-141 targets localize to different cellular components and function at various levels, forming distinct crosstalk and/or feedback loops, we propose that miR-141 precisely inhibits angiogenesis through a "3D" regulatory network (Fig. 6). Specifically, the secretory chemokine CXCL12β [23] and cytokine TGFβ2 [32] are extracellular targets, NRP1 is a cell membrane receptor [28], GAB1 is a docking protein [26], and GATA6 is an intracellular transcription factor [27] (Fig. 6). The cell membrane receptor NRP1 acts as a co-receptor of VEGF to potentiate VEGF/VEGFR2 signaling [28, 29]. After the receptors are activated, the signal is transduced to GAB1 with the help of GRB2, and subsequently stimulates downstream signaling to promote angiogenesis [26]. The chemokine CXCL12β binds primarily to CXCR4, a G-protein-coupled receptor, which couples with the heterotrimeric G-protein Gαβγ to stimulate angiogenesis [23]. TGFβs bind to TGFβ type II receptors and activate two distinct type I receptors, ALK1 and ALK5, in endothelial cells, which leads to biphasic effects in angiogenesis [32, 46]. It has been reported that the transcription factor GATA6 promotes angiogenesis by modulating TGFβ2 expression and the intricate balance between ALK1- and ALK5-dependent signaling [27]. Overall, these five miR-141 targets organize a kind of three-dimensional regulation

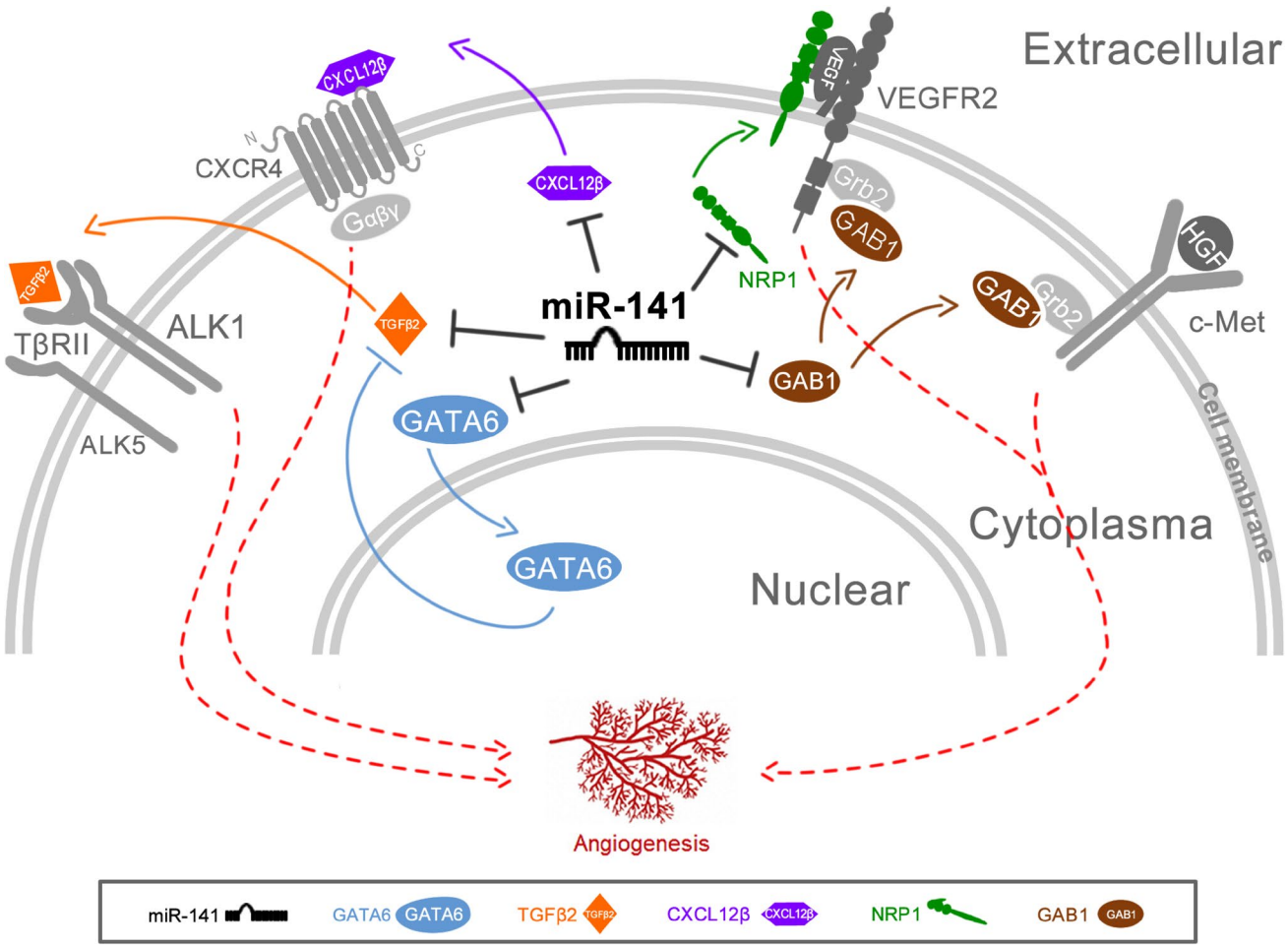


**Fig. 6** A schematic of the miR-141 regulatory network in angiogenesis. This schematic shows a network of angiogenesis-associated genes directly regulated by miR-141. Through this three-dimensional regulatory network, miR-141 inhibits angiogenesis by suppressing endothelial cell proliferation, migration, and tube formation

network to modulate different biological processes of angiogenesis. In the future, technical advance may allow us to simultaneously silence multiple target genes in HUVECs to precisely assess their contributions to this regulatory network.

Based on published data and our results, we posit that the function of miR-141 might vary across different situations and environments. In our study, we clearly showed that miR-141 has anti-angiogenic effects in endothelial cells. However, the environment inside a tumor is much more complicated than the experimental environment. First, the tumor cells themselves are heterogeneous; second, there are other cell types, such as macrophages, vessel endothelial cells, and tumor cell-derived endothelial cell-like cells, with elaborate cell–cell crosstalk. For example, findings from Kras-transformed fibroblasts [14] and NSCLC patients [15] indicate that miR-141 promotes angiogenesis. These pro-angiogenic effects may be related to miR-141 activity in the tumor cells and/or tumor microenvironments, rather than in the endothelial cells. Therefore, future work should explore the roles of miR-141 in tumor versus endothelial cells, in vasculogenic mimicry and angiogenesis, in cell–cell communication, and in tumors in situ and distal metastatic foci based on a single tumor model.

EMT and angiogenesis are two key processes that promote tumor growth and metastasis. Because all the members of the miR-200 family inhibit both processes, they have great potential to be developed as cancer therapeutic targets. One remaining challenge is that the miR-200 family members may function differently in local tumors versus distant metastatic foci. For example, there are several reports showing that the miR-200s enhance breast cancer cell colonization to form distant metastasis [47–49], so it might be necessary to adopt different strategies to treat tumors in situ and distal metastatic cancer.

**Acknowledgements** We appreciate Dr. Kerin Higa (City of Hope) and Dr. Wen Jin (Sigilon therapeutics) for critically reading the manuscript and for helpful discussions. This work was supported by the grants from the National Natural Science Foundation of China [Grant Numbers 31570786, 31600630 and 31770867] and the China Postdoctoral Science Foundation China [Grant Number 2016M591990].

## References

1. Folkman J (1971) Tumor angiogenesis: therapeutic implications. N Engl J Med 285(21):1182–1186
2. Carmeliet P (2005) Angiogenesis in life, disease and medicine. Nature 438(7070):932–936
3. De Palma M, Biziato D, Petrova TV (2017) Microenvironmental regulation of tumour angiogenesis. Nat Rev Cancer 17(8):457–474
4. Ha M, Kim VN (2014) Regulation of microRNA biogenesis. Nat Rev Mol Cell Biol 15(8):509–524
5. Bartel DP (2004) MicroRNAs: genomics, biogenesis, mechanism, and function. Cell 116(2):281–297
6. Fish JE, Srivastava D (2009) MicroRNAs: opening a new vein in angiogenesis research. Sci Signal 2(52):pe1
7. Wang W, Zhang E, Lin C (2015) MicroRNAs in tumor angiogenesis. Life Sci 136:28–35
8. Korpal M, Kang Y (2008) The emerging role of miR-200 family of microRNAs in epithelial-mesenchymal transition and cancer metastasis. RNA Biol 5(3):115–119
9. Mongroo PS, Rustgi AK (2010) The role of the miR-200 family in epithelial-mesenchymal transition. Cancer Biol Ther 10(3):219–222
10. Zhang HF, Xu LY, Li EM (2014) A family of pleiotropically acting microRNAs in cancer progression, miR-200: potential cancer therapeutic targets. Curr Pharm Des 20(11):1896–1903
11. Chan YC, Khanna S, Roy S, Sen CK (2011) miR-200b targets Ets-1 and is down-regulated by hypoxia to induce angiogenic response of endothelial cells. J Biol Chem 286(3):2047–2056
12. Bartoszewska S, Kochan K, Piotrowski A, Kamysz W, Ochocka RJ, Collawn JF, Bartoszewski R (2015) The hypoxia-inducible miR-429 regulates hypoxia-inducible factor-1alpha expression in human endothelial cells through a negative feedback loop. FASEB J 29(4):1467–1479
13. Ding Y, Hu Z, Luan J, Lv X, Yuan D, Xie P, Yuan S, Liu Q (2017) Protective effect of miR-200b/c by inhibiting vasohibin-2 in human retinal microvascular endothelial cells. Life Sci 191:245–252
14. Mateescu B, Batista L, Cardon M, Gruosso T, de Feraudy Y, Mariani O, Nicolas A, Meyniel JP, Cottu P, Sastre-Garau X, Mechta-Grigoriou F (2011) miR-141 and miR-200a act on ovarian tumorigenesis by controlling oxidative stress response. Nat Med 17(12):1627–1635
15. Tejero R, Navarro A, Campayo M, Vinolas N, Marrades RM, Cordeiro A, Ruiz-Martinez M, Santasusagna S, Molins L, Ramirez J, Monzo M (2014) miR-141 and miR-200c as markers of overall survival in early stage non-small cell lung cancer adenocarcinoma. PLoS ONE 9(7):e101899
16. Pecot CV, Rupaimoole R, Yang D, Akbani R, Ivan C, Lu C, Wu S, Han HD, Shah MY, Rodriguez-Aguayo C, Bottsford-Miller J, Liu Y, Kim SB, Unruh A, Gonzalez-Villasana V, Huang L, Zand B, Moreno-Smith M, Mangala LS, Taylor M, Dalton HJ, Sehgal V, Wen Y, Kang Y, Baggerly KA, Lee JS, Ram PT, Ravoori MK, Kundra V, Zhang X, Ali-Fehmi R, Gonzalez-Angulo AM, Massion PP, Calin GA, Lopez-Berestein G, Zhang W, Sood AK (2013) Tumour angiogenesis regulation by the miR-200 family. Nat Commun 4:2427
17. Weng C, Dong H, Chen G, Zhai Y, Bai R, Hu H, Lu L, Xu Z (2012) miR-409-3p inhibits HT1080 cell proliferation, vascularization and metastasis by targeting angiogenin. Cancer Lett 323(2):171–179
18. Mriouah J, Boura C, Thomassin M, Bastogne T, Dumas D, Faivre B, Barberi-Heyob M (2012) Tumor vascular responses to antivascular and antiangiogenic strategies: looking for suitable models. Trends Biotechnol 30(12):649–658
19. Malinda KM (2009) In vivo matrigel migration and angiogenesis assay. Methods Mol Biol 467:287–294
20. Agarwal V, Bell GW, Nam JW, Bartel DP (2015) Predicting effective microRNA target sites in mammalian mRNAs. Elife 4:e05005
21. Krek A, Grun D, Poy MN, Wolf R, Rosenberg L, Epstein EJ, MacMenamin P, da Piedade I, Gunsalus KC, Stoffel M, Rajewsky N (2005) Combinatorial microRNA target predictions. Nat Genet 37(5):495–500
22. Paraskevopoulou MD, Georgakilas G, Kostoulas N, Vlachos IS, Vergoulis T, Reczko M, Filippidis C, Dalamagas T, Hatzigeorgiou AG (2013) DIANA-microT web server v5.0: service

integration into miRNA functional analysis workflows. Nucleic Acids Res 41:W169–W173 (**Web Server issue**)
23. Salcedo R, Oppenheim JJ (2003) Role of chemokines in angiogenesis: CXCL12/SDF-1 and CXCR4 interaction, a key regulator of endothelial cell responses. Microcirculation 10(3–4):359–370
24. Song ZY, Wang F, Cui SX, Qu XJ (2018) Knockdown of CXCR4 inhibits CXCL12-induced angiogenesis in HUVECs through downregulation of the MAPK/ERK and PI3K/AKT and the Wnt/beta-catenin pathways. Cancer Investig 36(1):10–18
25. Shioyama W, Nakaoka Y, Higuchi K, Minami T, Taniyama Y, Nishida K, Kidoya H, Sonobe T, Naito H, Arita Y, Hashimoto T, Kuroda T, Fujio Y, Shirai M, Takakura N, Morishita R, Yamauchi-Takihara K, Kodama T, Hirano T, Mochizuki N, Komuro I (2011) Docking protein Gab1 is an essential component of postnatal angiogenesis after ischemia via HGF/c-met signaling. Circ Res 108(6):664–675
26. Laramee M, Chabot C, Cloutier M, Stenne R, Holgado-Madruga M, Wong AJ, Royal I (2007) The scaffolding adapter Gab1 mediates vascular endothelial growth factor signaling and is required for endothelial cell migration and capillary formation. J Biol Chem 282(11):7758–7769
27. Froese N, Kattih B, Breitbart A, Grund A, Geffers R, Molkentin JD, Kispert A, Wollert KC, Drexler H, Heineke J (2011) GATA6 promotes angiogenic function and survival in endothelial cells by suppression of autocrine transforming growth factor beta/activin receptor-like kinase 5 signaling. J Biol Chem 286(7):5680–5690
28. Koch S (2012) Neuropilin signalling in angiogenesis. Biochem Soc Trans 40(1):20–25
29. Kofler NM, Simons M (2015) Angiogenesis versus arteriogenesis: neuropilin 1 modulation of VEGF signaling. F1000Prime Rep 7:26
30. Iwatsuki K, Tanaka K, Kaneko T, Kazama R, Okamoto S, Nakayama Y, Ito Y, Satake M, Takahashi S, Miyajima A, Watanabe T, Hara T (2005) Runx1 promotes angiogenesis by downregulation of insulin-like growth factor-binding protein-3. Oncogene 24(7):1129–1137
31. Sangpairoj K, Vivithanaporn P, Apisawetakan S, Chongthammakun S, Sobhon P, Chaithirayanon K (2017) RUNX1 regulates migration, invasion, and angiogenesis via p38 MAPK pathway in human glioblastoma. Cell Mol Neurobiol 37(7):1243–1255
32. Goumans MJ, Lebrin F, Valdimarsdottir G (2003) Controlling the angiogenic switch: a balance between two distinct TGF-b receptor signaling pathways. Trends Cardiovasc Med 13(7):301–307
33. Liao KH, Chang SJ, Chang HC, Chien CL, Huang TS, Feng TC, Lin WW, Shih CC, Yang MH, Yang SH, Lin CH, Hwang WL, Lee OK (2017) Endothelial angiogenesis is directed by RUNX1T1-regulated VEGFA, BMP4 and TGF-beta2 expression. PLoS ONE 12(6):e0179758
34. Huang Z, Shi T, Zhou Q, Shi S, Zhao R, Shi H, Dong L, Zhang C, Zeng K, Chen J, Zhang J (2014) miR-141 Regulates colonic leukocytic trafficking by targeting CXCL12beta during murine colitis and human Crohn's disease. Gut 63(8):1247–1257
35. Burk U, Schubert J, Wellner U, Schmalhofer O, Vincan E, Spaderna S, Brabletz T (2008) A reciprocal repression between ZEB1 and members of the miR-200 family promotes EMT and invasion in cancer cells. EMBO Rep 9(6):582–589
36. Feng J, Xue S, Pang Q, Rang Z, Cui F (2017) miR-141-3p inhibits fibroblast proliferation and migration by targeting GAB1 in keloids. Biochem Biophys Res Commun 490(2):302–308
37. Lu Y, Xiong Y, Huo Y, Han J, Yang X, Zhang R, Zhu DS, Klein-Hessling S, Li J, Zhang X, Han X, Li Y, Shen B, He Y, Shibuya M, Feng GS, Luo J (2011) Grb-2-associated binder 1 (Gab1) regulates postnatal ischemic and VEGF-induced angiogenesis through the protein kinase A-endothelial NOS pathway. Proc Natl Acad Sci USA 108(7):2957–2962
38. Murga M, Fernandez-Capetillo O, Tosato G (2005) Neuropilin-1 regulates attachment in human endothelial cells independently of vascular endothelial growth factor receptor-2. Blood 105(5):1992–1999
39. Heidemann J, Ogawa H, Rafiee P, Lugering N, Maaser C, Domschke W, Binion DG, Dwinell MB (2004) Mucosal angiogenesis regulation by CXCR4 and its ligand CXCL12 expressed by human intestinal microvascular endothelial cells. Am J Physiol Gastrointest Liver Physiol 286(6):G1059–G1068
40. Gao Y, Feng B, Han S, Zhang K, Chen J, Li C, Wang R, Chen L (2016) The roles of MicroRNA-141 in human cancers: from diagnosis to treatment. Cell Physiol Biochem 38(2):427–448
41. Choi YC, Yoon S, Jeong Y, Yoon J, Baek K (2011) Regulation of vascular endothelial growth factor signaling by miR-200b. Mol Cells 32(1):77–82
42. Sinha M, Ghatak S, Roy S, Sen CK (2015) microRNA-200b as a switch for inducible adult angiogenesis. Antioxid Redox Signal 22(14):1257–1272
43. Chuang TD, Panda H, Luo X, Chegini N (2012) miR-200c is aberrantly expressed in leiomyomas in an ethnic-dependent manner and targets ZEBs, VEGFA, TIMP2, and FBLN5. Endocr Relat Cancer 19(4):541–556
44. Shi L, Zhang S, Wu H, Zhang L, Dai X, Hu J, Xue J, Liu T, Liang Y, Wu G (2013) MiR-200c increases the radiosensitivity of non-small-cell lung cancer cell line A549 by targeting VEGF-VEGFR2 pathway. PLoS ONE 8(10):e78344
45. Bartel DP (2009) MicroRNAs: target recognition and regulatory functions. Cell 136(2):215–233
46. Lebrin F, Deckers M, Bertolino P, Ten Dijke P (2005) TGF-beta receptor function in the endothelium. Cardiovasc Res 65(3):599–608
47. Dykxhoorn DM, Wu Y, Xie H, Yu F, Lal A, Petrocca F, Martinvalet D, Song E, Lim B, Lieberman J (2009) miR-200 enhances mouse breast cancer cell colonization to form distant metastases. PLoS ONE 4(9):e7181
48. Korpal M, Ell BJ, Buffa FM, Ibrahim T, Blanco MA, Celia-Terrassa T, Mercatali L, Khan Z, Goodarzi H, Hua Y, Wei Y, Hu G, Garcia BA, Ragoussis J, Amadori D, Harris AL, Kang Y (2011) Direct targeting of Sec23a by miR-200 s influences cancer cell secretome and promotes metastatic colonization. Nat Med 17(9):1101–1108
49. Le MT, Hamar P, Guo C, Basar E, Perdigao-Henriques R, Balaj L, Lieberman J (2014) miR-200-containing extracellular vesicles promote breast cancer cell metastasis. J Clin Investig 124(12):5109–5128